Int. J. Electrochem. Sci., 11 **(2016)** 10436 – 10448, doi: 10.20964/2016.12.51

International Journal of ELECTROCHEMICAL SCIENCE
www.electrochemsci.org

Oxygen Reduction on Au(100)-like Polycrystalline Gold Electrode in Alkaline Solution

Irina Srejić[1], *Milutin Smiljanić*[1], *Zlatko Rakočević*[1], *Svetlana Štrbac*[2,*]

[1] INS Vinča, Laboratory of Atomic Physics, University of Belgrade, Mike Alasa 12-14, 11001 Belgrade, Serbia
[2] ICTM-Institute of Electrochemistry, University of Belgrade, Njegoševa 12, 11000 Belgrade, Serbia
[*]E-mail: sstrbac@tmf.bg.ac.rs

Received: 17 September 2016 / *Accepted:* 10 October 2016 / *Published:* 10 November 2016

Catalytic properties of polycrystalline gold, Au(poly), were examined for the oxygen reduction reaction in alkaline solution using the rotating disc electrode technique. On electrochemically prepared Au(poly), oxygen reduction proceeds partly through 4e-reaction pathway resembling the activity of bare Au(100) in alkaline solution. Electrochemical behavior of such Au(100)-like polycrystalline gold electrode was compared with bare Au(100) surface, as well as with stepped Au(210)=Au[2(100)x(110)] and Au(533)=Au[4(111)x(100)] surfaces. It is shown that polycrystalline gold electrode behaved in a similar manner as stepped Au[n(111)x(100)] surfaces, meaning that the enrichment in (111)x(100) steps, rather than in (100) orientation is responsible for a partial 4e-reaction pathway in alkaline solution.

Keywords: Au(poly), Au(100), AFM, RDE, oxygen reduction, alkaline solution

1. INTRODUCTION

Oxygen reduction reaction (ORR) is one of the most extensively studied electrochemical reactions because of its importance in fuel cells, corrosion, and industrial processes [1,2]. Although ORR has been studied earlier on polycrystalline gold, Au(poly), [3,4], the comprehensive studies on single crystals with various orientations [5-12], enabled the most detailed insight into the reaction kinetics and mechanism. These studies have shown that oxygen reduction reaction on gold is sensitive towards surface structure, anion adsorption and pH of the solution. While in acid solution ORR proceeds on all single crystal gold surfaces with the exchange of 2e [8,9], in alkaline solution its mechanism depends strongly on the crystallographic orientation [5-7]. Among all gold single crystals

with various orientations, the Au(100) surface has shown the best catalytic activity for ORR in alkaline solutions, which proceeds with the exchange of 4e, in contrast to the Au(111) and Au(110), whose activity is similar to that of a polycrystalline Au and proceeds with the exchange of 2e [5,6,8]. Similarly, on Au single crystal surfaces vicinal to (100), which are composed of wide terraces of (100) orientation, ORR proceeds mainly through 4e-pathway due to the presence of a significant amount of (100) surface sites [8,10,11]. It has also been shown that on those stepped surfaces, which are composed of (100)x(111) steps, ORR proceeds at least partly through 4e-reduction, the fraction of which depends on the width of (100) terraces [7,8,11], while on those with (100)x(110) [8,11], or (111)x(111) steps [12], only 2e-reaction pathway is operative.

It has been reported that depending on the pretreatment of polycrystalline Au surface, ORR in alkaline solution might either proceed through 2e-reduction pathway, or at least partly through 4e-reduction pathway like Au(100) single crystal, which was demonstrated for gold thin films obtained by the evaporation of gold on glassy carbon substrate [13]. Au(100)-like behavior towards ORR can be achieved either by cycling the potential from the onset of hydrogen evolution to an anodic limit just below the onset of the oxide region in oxygen saturated 1 M NaOH or by holding the surface at a potential of mild hydrogen evolution in argon saturated acid solution [14]. Although there is no a definite answer about the origin of such behavior, the first assumption would be that the enrichment in (100) surface sites is responsible for Au(100)-like behavior for ORR in alkaline solution. Such assumption would be consistent with the reports on the gold nanoparticles and polycrystalline gold enriched either in the (111) facets, which have been prepared in the presence of iodide ions [15,16] or in the (100) and (110) facets prepared in the presence of cysteine [15,17]. We have also found recently that, after a prolonged treatment by electrochemical polishing, which involved hydrogen evolution, bulk polycrystalline gold electrode exhibited higher catalytic activity for ORR in 0.1 M $HClO_4$ solution than previously reported [18].

Having in mind the significance and a widespread use of polycrystalline gold electrode in electrocatalysis generally, the purpose of this work is to demonstrate that its surface structure cannot be taken unambiguously, but that it can be tuned by a proper choice of the electrode preparation. Instead of widely used mechanical polishing, we have explored the effect of the additional electrochemical polishing, which is also widely used for a final surface preparation in order to provide smooth and clean electrode surface. We have examined as prepared polycrystalline gold electrode for the study of ORR in alkaline solution. Due to the importance of hydrogen peroxide as a possible reaction intermediate, both hydrogen peroxide oxidation and reduction reactions (HPOR/HPRR), were also examined. In order to find out the origin of the high activity for ORR of so called Au(100)-like polycrystalline gold electrode, its behavior was compared to the behavior of bare Au(100) and of stepped Au(210) and Au(533) single crystal electrodes. Therefore, the assumption that the enrichment in (100) surface sites is responsible for Au(100)-like behavior of polycrystalline gold electrode surface has been challenged by comparison with the behavior of stepped surfaces which are enriched in (100)x(111) or in (100)x(110) step sites. The mechanism of ORR on Au(100)-like polycrystalline gold electrode has been reexamined with respect to the geometry of predominant surface sites.

2. EXPERIMENTAL

2.1. Preparation of Au(poly) and Au(100) surfaces

Au(poly) disc (Pine Instruments Co.), 5 mm in diameter, and Au(100), Au(210) and Au(533) single crystal electrodes (Metal Crystal Ltd. Co, Cambridge, England), 8 mm in diameter, mounted in teflon holder were used as working electrodes for electrochemical measurements. Au(poly) and Au(100) (MaTeck, Jullich), 12 mm in diameter were used for ex situ AFM characterization. Electrodes were cleaned by electrochemical polishing before each experiment, which involved anodic oxidation in 1 M perchloric acid solution, the chemical removal of gold oxide by its dissolution in 10% HCl solution, and subsequent removal of the traces of chloride by a mild cathodic hydrogen evolution in 1 M perchloric acid solution. Single crystal Au(100) electrode was additionally annealed using butane flame for AFM measurements.

2.2. AFM characterization of Au(poly) and Au(100) surfaces

The surface structure of Au(poly) and Au(100) electrodes were characterized *ex situ* using Atomic Force Microscopy (Multimode quadrex SPM with Nanoscope IIIe controller, Veeco Instruments, Inc.) operating in tapping mode with a commercial Veeco RFESP AFM probe (NanoScience Instruments, Inc.). Root mean square (RMS) roughness, which is defined as the square deviation of an analyzed surface from the ideal one was estimated from surface topography AFM images using Veeco subprogram.

2.3. Electrochemical measurements

Electrochemical characterization involved cyclic voltammetry in deaerated 0.1 M NaOH solution. Catalytic properties of gold electrodes were examined by Linear Sweep Voltammetry (LSV) using the rotating disc electrode (RDE) method. Oxygen reduction reaction measurements were performed in oxygen saturated 0.1 M NaOH, while hydrogen peroxide oxidation and reduction reactions measurements were performed in oxygen free 0.1 M NaOH solution containing 5 mM H_2O_2. LSV curves for both ORR and HPRR/HPOR were recorded in the cathodic direction starting from the potential of 0.2 V down to -0.8 V.

2.4. Chemicals

Solutions for electrochemical polishing were prepared from $HClO_4$ (Merck) and HCl (Merck), while working solutions were prepared from NaOH (Merck), all diluted with Milli-pure water. Working solutions were either deoxygenated with 99.999 % N_2 (Messer), or oxygenated by purging 99.999 % O_2 (Messer). Pt wire and Ag/AgCl, 3M KCl were used as counter and reference electrodes, respectively. All measurements were performed at room temperature.

3. RESULTS AND DISCUSSION

3.1. Oxygen reduction on Au(100)-like polycrystalline gold and comparison with ORR on bare Au(100) in alkaline solution

It has been reported earlier that ORR on polycrystalline gold in alkaline solution proceeds through the exchange of 2e [3,4,13]. It has also been reported that depending on the preparation, it could become more active, meaning that the ORR might proceed also through 4e-reaction pathway like Au(100), thus earning the name Au(100)-like polycrystalline gold [13,14]. The electrochemical preparation explored in this work also as a result gives active, Au(100)-like polycrystalline gold electrode. To illustrate the similarity in the activity of such prepared Au(poly) and well known activity of bare Au(100) [5,10], the polarization curves for ORR on both electrodes, are presented in Figure 1. Reaction scheme for ORR in alkaline solution as provided in refs. [5,10], will be used for the analysis of ORR pathways.

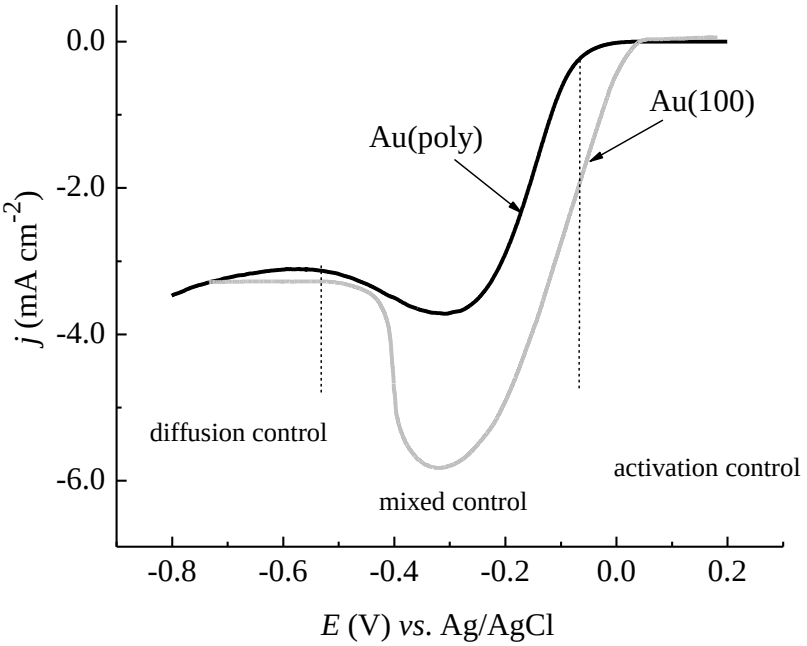

Figure 1. Polarization curves for ORR on Au(100)-like Au(poly) and bare Au(100) recorded in oxygen saturated 0.1 M NaOH for the same rotation rate of ω = 1600 rpm, and at a sweep rate of 50 mV/s.

In the potential region starting at the initial potential of approx. 0.0 V down to approx. -0.5 V (activation and mixed control), the obtained current density is higher than the limiting current density at potentials lower than -0.5 V (diffusion control) corresponding to the exchange of 2e. This indicates that ORR proceeds partly through 4e-reaction pathway just like on bare Au(100) in the potential region from -0.0 V down to -0.5 V. Such similarity in the activity towards ORR in alkaline solution between Au(100)-like Au(poly) and bare Au(100) suggests that during the electrochemical preparation of Au(poly), it might become enriched in (100) surface domains. Is there really the enrichment of

Au(poly) in (100) surface domains, which would be responsible for its activity? To answer that question, surface morphology and CV curves of Au(100)-like Au(poly) and of bare Au(100) are compared.

3.2. Comparison of AFM images and CV curves of Au(100)-like Au(poly) and bare Au(100) surfaces

Au(poly) electrode surface was characterized *ex situ* by AFM and electrochemically by cyclic voltammetry, and results are presented in Figure 2. For comparison, corresponding results for single crystal Au(100) surface are also presented.

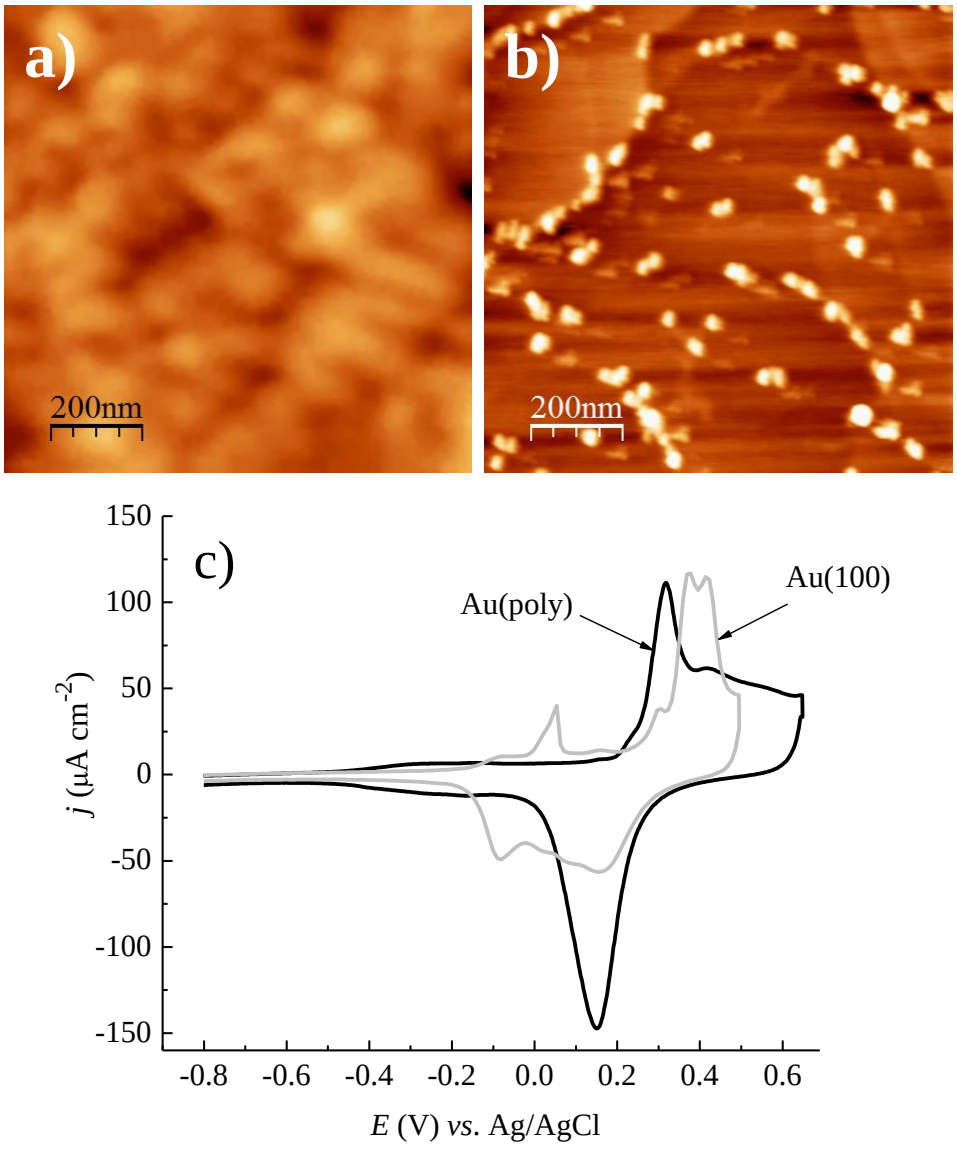

Figure 2. a) AFM image (1 x 1) □m^2 of: a) Au(poly), z-scale = 8.3 nm, RMS roughness 0.95; b) Au(100), z-scale = 4.5 nm, RMS roughness 0.7; c) CVs of the same surfaces recorded in deaerated 0.1 M NaOH at a sweep rate of 50 mV/s.

Surface topography AFM image of Au(poly), Figure 2 (a), shows that the surface consists of many facets which can be identified by a lighter color of distinguished surface domains, the boundaries of which are clearly defined by a darker color. In contrast to this, AFM image of Au(100) surface, Figure 2 (b), shows several hundred nanometers wide terraces clearly separated by steps. Square-shaped gold islands situated mainly along step edges are observed on Au(100) surface due to the lifting of surface reconstruction thermally induced during annealing. Presence of monolayer high gold islands, which were formed due to the lifting of electrochemically induced surface reconstruction was first observed by *in situ* Scanning Tunneling Microscopy [19,20].

Cyclic voltammetry curves of Au(poly) and Au(100) recorded over a wider potential region, including double layer and oxide formation/reduction, Figure 2 (c), show a significant difference between the two electrodes. For Au(poly), the preoxidation potential region corresponding to the specific adsorption/desorption of OH^- anions from approx. -0.5 V up to 0.2 V, proceeds as a reversible process. At potentials higher than 0.2 V, the oxide formation begins in the forward scan. The main oxide formation peak is centered at 0.36 V, while in the reverse scan a corresponding irreversible reduction peak is centered at 0.15 V. The behavior of Au(100) surface is quite different. Namely, the specific OH^- adsorption begins at -0.15 V and proceeds up to the beginning of oxide formation at 0.3 V, showing a characteristic sharp peak due to the lifting of surface reconstruction at 0.05 V. Both OH^- adsorption/desorption, and oxide formation/reduction are irreversible processes on Au(100) [10,11,21]. The obvious differences in the shape of CV curves for Au(poly) and Au(100) in alkaline solution strongly underline the differences in their surface structure, meaning that any significant fraction of (100) surface domains, or (100) surface areas on Au(poly) cannot be identified from CV curves. Both surface topography and CV curves suggest that there is no enrichment in (100) surface domains, and that instead the generation of surface sites with the other geometry is responsible for the enhanced activity of Au(poly) towards ORR. Therefore, the electrochemical behavior of Au(100)-like Au(poly) was additionally compared with the behavior of different stepped single crystal gold surfaces and results presented below.

3.3. Comparison of CV curves and ORR activity of Au(100)-like Au(poly) and stepped Au single crystals

CV curve of Au(100)-like Au(poly) is compared to CV curves of stepped single crystal gold surfaces with different step orientation: Au(533) = [4(111)x(100)] and Au(210) = [2(100)x(110)], and obtained results are presented in Figure 3. CV of Au(100) is presented again for comparison. CV curve of Au(210) is in agreement with previously published [11,21], as well as the one for Au(533) [11]. Comparing CV curve of Au(poly) with the ones for Au(210) and Au(533), it can be seen that although similar to both, it fits more Au(533) orientation, with respect to the intensity of peaks corresponding to OH^-adsorption/desorption and oxide formation. Again, it can be clearly seen that the CV curve for bare Au(100) single crystal differs significantly from Au(poly) and from both examined stepped surfaces. It point out to the enrichment of Au(poly) with steps of either (100)x(111) orientation as on Au(533) or (100)x(110) orientation as in Au(210).

According to the previous comprehensive study of ORR on Au(100) and on various stepped surface in alkaline solution [8,11], OH^- specific adsorption has a crucial role for 4e-reaction pathway. Therefore, CV curves recorded in deaerated 0.1 M NaOH solution for all examined gold electrodes in the potential region of OH^- specific adsorption, and polarization curves recorded using RDE technique for the same rotation rate in oxygen saturated 0.1 M NaOH solution, are presented together in Figure 4.

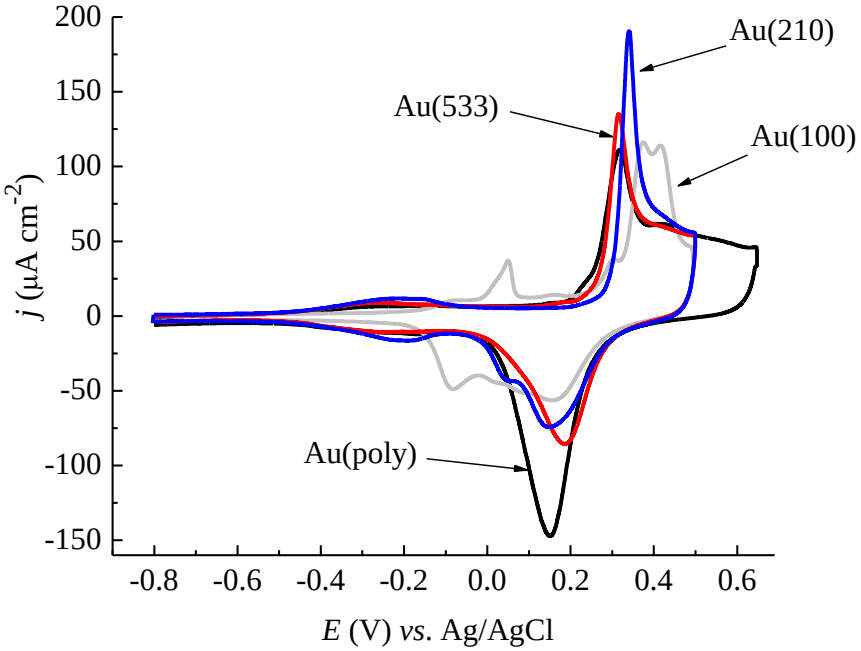

Figure 3. CVs of Au(poly), Au(100), Au(210) and Au(533) surfaces recorded in 0.1 M NaOH at a sweep rate of 50 mV/s.

It can be seen from Figure 4 (a), that OH^- adsorption/desorption occurs as a reversible process in the same potential region, although not exactly in the same extent on Au(poly), Au(533) and Au(210), while on Au(100) it proceeds in a different manner as described above. This again excludes the presence of (100) domains on Au(poly) as responsible for a partial 4e-reduction on Au(poly), but instead points out to the presence of different steps on Au(210)=[2(100)x(111)] and Au(533)=[4(111)x(100)]. Despite the fact that both (100)x(111) and (110)x(111) steps are susceptible for OH^- chemisorption, they behave differently towards oxygen reduction, as can be seen from Figure 4 (b). It has been reported that on all stepped surfaces having (111)x(110) steps, ORR proceeds only through 2e-reaction pathway [8,11], which is consistent with polarization curve obtained presented in Figure 4 (b) for Au(210). It has also been reported that on all stepped surfaces having (100)x(111), ORR proceeds at least partly through 4e-reaction pathway [7,8,11] which is consistent with polarization curve for Au(533) from Figure 4 (b). According to these findings, it is reasonable to assume that Au(100)-like Au(poly) electrode used in this work, being active partly for 4e-reaction is enriched in (111)x(100) steps, just like Au(533), and that those particular steps are responsible for its Au(100)-like behavior.

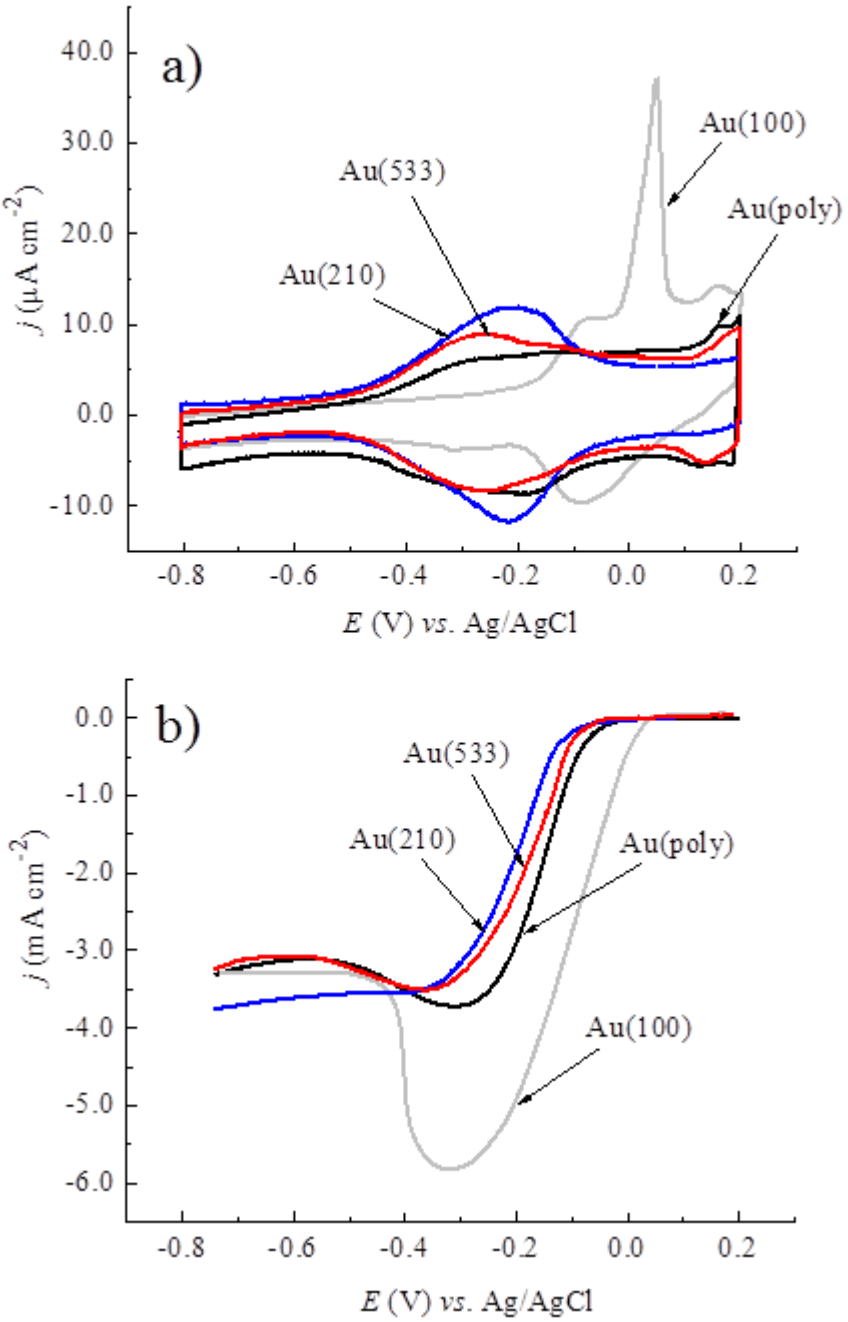

Figure 4. Comparison of Au(poly), Au(100) and stepped Au(533) and Au(210) surfaces: a) CVs in 0.1 M NaOH; b) Polarization curves for ORR on rotating electrodes in oxygen saturated 0.1 M NaOH solution for the same rotation rate of ω = 1600 rpm, and at a sweep rate of 50 mV/s.

The presence of (100)x(111) steps can also explain the hereby obtained shift of the onset of the ORR towards more positive potentials than those expected for ORR on polycrystalline gold [7,14]. The onset potential for ORR of approx. 0.0 V is in accordance with previously reported [11], where ORR was studied on similar Au(100)-like polycrystalline gold surface. The current density increases in the potential region of specifically adsorbed OH^- anions coinciding with both the activation and mixed

control regions (see Figure 1), while at lower potentials, where OH^- anions are desorbed, the oxygen reduction proceeds with the lowest current density, which coincides with the diffusion control.

3.4. Oxygen reduction and hydrogen peroxide reduction/oxidation Au(100)-like Au(poly) electrode

The reaction mechanism of ORR on Au(100)-like Au(poly) is reexamined in detail having in mind the conclusions above that there is most likely the enrichment of polycrystalline gold surface with (100)x(111) steps. Polarization curves for ORR as well as for hydrogen peroxide reduction/oxidation as a possible reaction intermediate, recorded in cathodic direction for six rotation rates are shown in Figure 5.

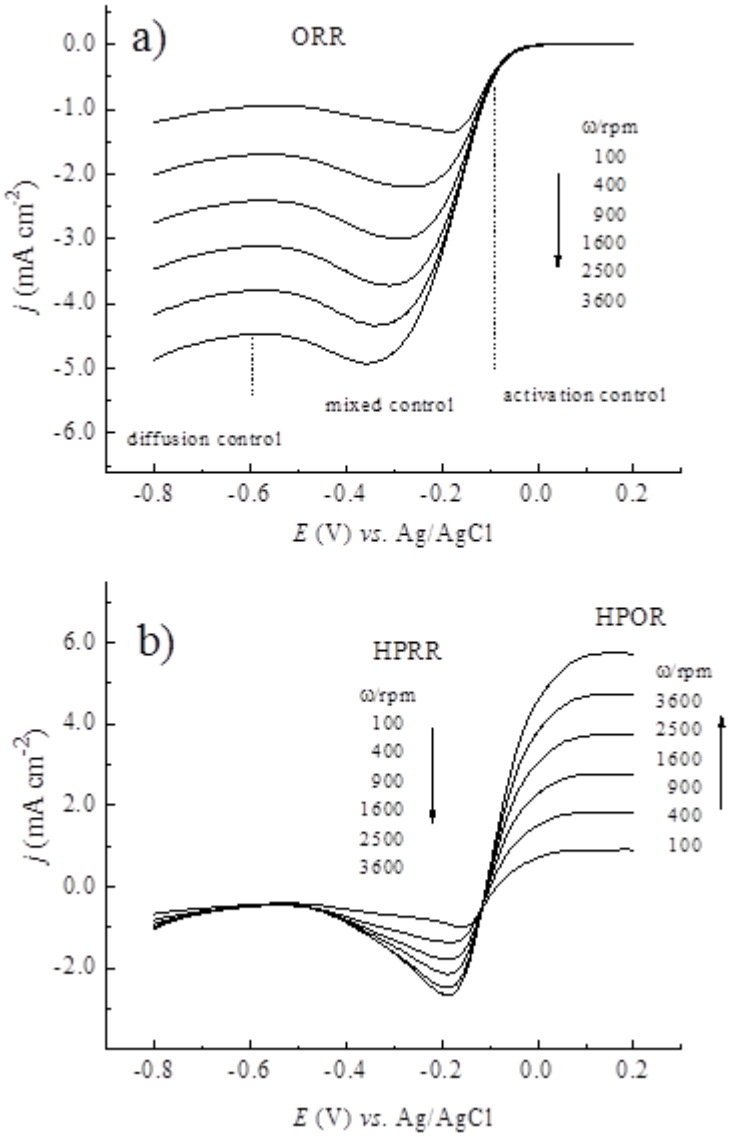

Figure 5. Polarization curves for: a) ORR on a rotating Au(poly) electrode in oxygen saturated 0.1 M NaOH solution; b) HPRR/HPOR in oxygen free 0.1 M NaOH solution containing 5 mM H_2O_2, obtained for various rotation rates with the potential scan rate of 50 mV/s.

From polarization curves for ORR on Au(100)-like Au(poly) electrode, Figure 5 (a), potential regions where the reaction proceeds under the activation control (not rotation rate dependent), mixed control (becomes rate dependent) and diffusion control (rate dependent) can be clearly separated. On the other hand, polarization curves for HPRR/HPOR, presented in Figure 5 (b), show mixed potential regions (rate dependent), which both coincide with the activation and mixed control regions for ORR. On the other hand, diffusion control (rate dependent) exists only for HORR at higher potentials (which are not of interest for ORR and will not be discussed further), while for HPRR there is no rotation rate dependent diffusion control at potentials corresponding to the diffusion control for ORR. The later suggests that in the diffusion control, ORR proceeds through 2e-reduction giving hydrogen peroxide as a product, which is consistent with the absence of OH^- anions on the Au(100-like Au(poly) electrode surface (see Figure 4 (a)), and its subsequent inactivity of the hydrogen peroxide further reduction. The activation and mixed potential regions for ORR in comparison with HPRR/HPOR will be analyzed in detail below.

In the activation control potential region for ORR, from comparison of the polarization curves for ORR and HPRR/HPOR, it can be seen that the onset potentials for ORR and HPRR differ for approx. 0.1 V. In that potential region, from 0.0 to -0.1 V, hydrogen peroxide undergoes the oxidation, indicating that oxygen reduction occurs either partly through $2e^-$ reaction pathway, and that produced hydrogen peroxide is being oxidized, or through a direct 4e-reduction, without the production of hydrogen peroxide as an intermediate. The later one seems more likely according to the previous findings using rotating ring-disc technique for ORR on Au(100) and its vicinal surface [10] as well as on Au(311)=[2(111)x(100)] [7]. Here we propose that the presence of those particular (111)x(100) steps is crucial for the specific adsorption of OH^- anions (see Figure 4 (a)), which act as a precursor for the dissociative adsorption of O_2, facilitating thus 4e-direct reaction pathway without the formation of hydrogen peroxide, which is in accordance with the findings from refs [7,10].

In the mixed control region, starting from -0.1 down to -0.35 V, oxygen reduction coincides with hydrogen peroxide reduction, indicating that ORR occurs predominantly through 4e-series pathway. In the potential region from -0.35 V down to -0.6 V, the current density for both ORR and HPRR decreases indicating that reaction mechanism changes from 4e- to 2e- pathway. Koutecky–Levich analysis of ORR in the mixed control region, enable the estimation of the number of electrons exchanged in the dependence of the potential and an insight into the rate determining steps.

Koutecky–Levich, (K-L), plots are constructed when the inverse current density (1/j) is plotted as a function of the inverse of the square root of the rotation rate ($\omega^{-1/2}$). RDE data were analyzed using a K-L equation:

$$1/j = 1/j_k + 1/j_l = 1/j_k + 1/B\omega^{1/2} \quad (1)$$

where: j is the measured current density, j_k and j_l are the kinetic and the diffusion-limited current densities, respectively, ω is the rotation rate (rad s^{-1}) and B is a constant which can be expressed as:

$$B = 0.62nFc(O_2)D(O_2)^{2/3}\nu^{-1/6} \quad (2)$$

where: F is Faraday's constant (96485 C mol^{-1}), $c(O_2)$ is the oxygen solubility (1.22×10^{-3} mol L^{-1} in 0.1 M NaOH), $D(O_2)$ is the oxygen diffusivity (1.90×10^{-5} cm^2 s^{-1} in 0.1 M NaOH), ν is the kinematic viscosity of the electrolyte (0.01 cm^2 s^{-1}) [22] and n is the overall number of electrons exchanged

which is calculated from Equation (2), using the experimental values of the slopes, 1/B. K–L plots and number of electrons exchanged are presented in Figure 6.

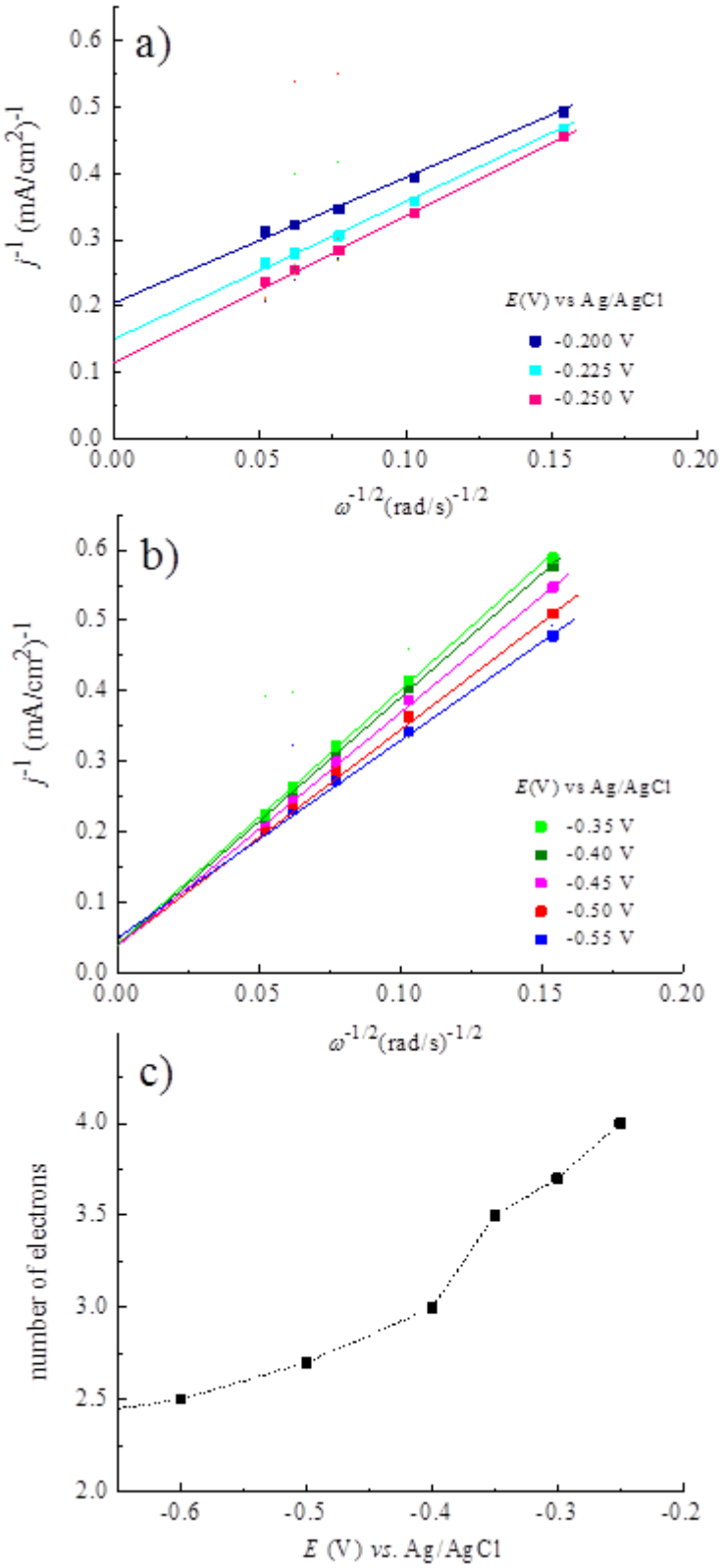

Figure 6. Koutecky–Levich plots obtained from the data from Figure 5 (a): a) for lower overpotentials; b) for higher overpotentials; c) number of electrons exchanged during ORR.

K-L plots, presented separately in Figure 6, for two potential regions to avoid overlapping, are straight lines, meaning that the reaction is first order in all cases, but they are not parallel indicating that the overall number of electrons exchanged changes with potential. The overall number of electrons exchanged as a function of the electrode potential, estimated from K-L plots, Figure 6 (c), clearly shows that the reaction turns from 4e-series at lower overpotential to 2e-series at higher overpotentials.

Tafel plot, defined as a function of the gradient of the potential vs. kinetic current gradient ($\Delta E/\Delta \log jk$), for ORR on Au(100)-like Au(poly) is given in Figure 7.

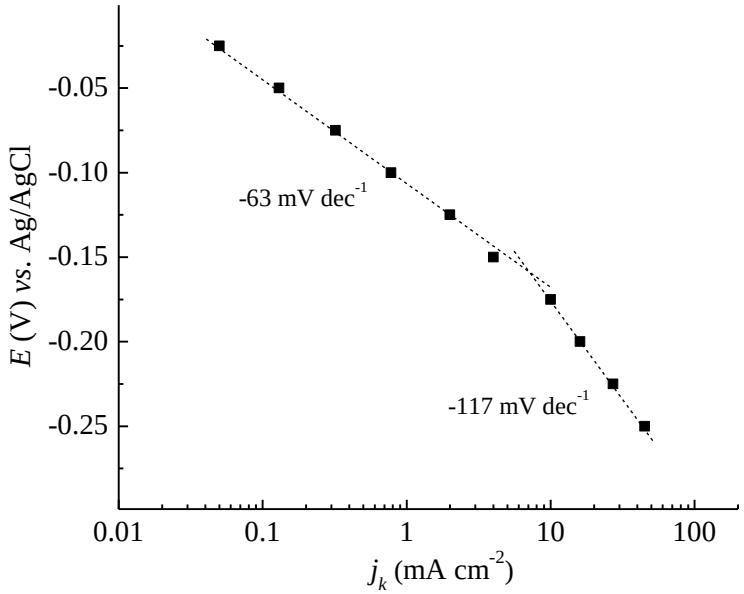

Figure 7. Tafel plot obtained using the data from ORR polarization curves from Figure 5 (a); j_k is taken as the average value for six rotation rates.

The obtained Tafel slope changes with potential in the activation control region. For lower overpotentials, the obtained slope of -63 mV per decade is close to the value of -60 mV per decade obtained for (100)-like polycrystalline gold electrode, mining that the diffusion of adsorbed O_2 is the rate-determining step [14], followed by the dissociative adsorption of O_2 and 4e-direct reduction, which is in agreement with the discussion above about the role of (111)x(100) steps. The lower value of Tafel slope on polycrystalline Au disk electrode is also reported in ref. [4]. Similarly, the smaller value of the Tafel slope (−52 mV per decade) was found for ORR on Au(poly) in Rb^+-containing 0.1 M NaOH solution at low overpotentials, where a complete 4e-reduction indicated that the reaction most likely proceeded through a direct pathway excluding the exchange of the first electron as the rate determining step [23]. For higher overpotentials, the obtained slope of -117 mV per decade is in accordance with a value of -120 mV per decade for single crystals [7,10] or polycrystalline Au electrode in alkaline solutions [3], indicating the exchange of the first electron as the rate determining step in 4e-series reduction pathway.

A complex behavior of hereby used Au(100)-like Au(poly) towards ORR in alkaline solution depending of the overpotential has been demonstrated, and the role of (111)x(100) steps explained.

4. CONCLUSIONS

Surface topography AFM images as well as CV curves have shown significant differences between Au(poly) and Au(100) surfaces, excluding the enrichment in (100) orientation on Au(poly) surface as a reason for its Au(100)-like activity for ORR. On the other hand, both CV curves recorded in oxygen free, and polarization curves for ORR recorded in oxygen saturated 0.1 M NaOH on several stepped Au single crystals, have shown that such Au(100)-like polycrystalline gold electrode behaves in a manner similar to Au[n(111)x(100)] stepped surfaces, meaning that its facets are rich in (111)x(100) steps. It has been shown that the presence of these steps, rather than the enrichment in (100) orientation is responsible for the enhanced activity of Au(poly) for ORR in alkaline solution.

ACKNOWLEDGEMENT
This work was financially supported by the Ministry of Science of the Republic of Serbia; project N^{o} 45005.

References

1. R.R. Adžić, in *Electrocatalysis*, J. Lipkowski, P.N. Ross (Eds), Wiley-VCH, New York, (1998) p.197.
2. X. Ge, A. Sumboja, D. Wuu, T. An, B. Li, F.W.T. Goh, T.S.A. Hor, Y. Zong, Z. Liu, *ACS Catal.* 5 (2015) 4643.
3. R. W. Zurilla, R. K. Sen, E. Yeager, *J. Electrochem. Soc.* 125 (1978) 1103.
4. A. Damjanović, M.A. Genshaw, J.O'M. Bockris, *J. Electroanal. Chem.* 15 (1967) 173.
5. R.R. Adžić, N.M. Marković, V.B. Vešović, *J. Electroanal. Chem.* 165 (1984) 105.
6. N.M. Marković, R.R. Adžić, V.B. Vešović, *J. Electroanal. Chem.* 165 (1984) 121.
7. N.A. Anastasijević, S. Štrbac, R.R. Adžić, *J. Electroanal. Chem.* 240 (1988) 239.
8. S. Štrbac, N.A. Anastasijević, R.R. Adžić, *Mater. Chem. Phys.* 22 (1989) 349.
9. S. Štrbac, R.R. Adzić, *J. Serb. Chem. Soc.* 57 (1992) 835.
10. S. Štrbac, N.A. Anastasijević, R.R. Adžić, *J. Electroanal. Chem.* 323 (1992) 179.
11. S. Štrbac, R.R. Adžić, *J. Electroanal. Chem.* 403 (1996) 169.
12. S. Štrbac, R.R. Adžić, *Electrochim. Acta* 41 (1996) 2903.
13. C.Paliteiro, A. Hamnett, J.B. Goodenough, *J. Electroanal. Chem.* 234 (1984) 193.
14. C. Paliteiro, *Electrochim. Acta* 39 (1994) 1633.
15. M. S. El-Deab, T. Sotomura, T. Ohsaka, *J. Electrochem. Soc.* 152 (2005) C1.
16. M.R. Miah, T. Ohsaka, *J. Electroanal. Chem.* 633 (2009) 71.
17. M.I. Awad, T. Ohsaka, *J. Power Sources,* 226 (2013) 306.
18. I. Srejić, M. Smiljanić, B. Grgur, Z. Rakočević, S. Štrbac, *Electrochim. Acta* 64 (2012) 140-146.
19. O.M. Magnussen, J. Hotlos, R.J. Behm, N. Batina, D.M. Kolb, *Surf. Sci.* 296 (1993) 310.
20. X. Gao, G.J. Edens, A. Hamelin, M.J. Weaver, *Surf. Sci.* 296 (1993) 333.
21. A. Hamelin, M.J. Sottomayor, F. Silva, S-C. Chang, M.J. Weaver, *J. Electroanal. Chem.* 295 (1990) 291.
22. J. Zagal, P. Bindra, E. Yeager, *J. Electrochem. Soc.* 127 (1980) 1506.
23. K. Kajii, T. Ohsaka, F. Kitamura, *Electrochem. Commun.* 12 (2010) 970.